



**HAL**  
open science

## Interface Characterization by Nanoindentation and EBSD of Cu/Cu and Al/Cu Joints Produced by Magnetic Pulse Welding (MPW)

Benjamin Zielinski, Tarik Sadat, Rudy Dubois, José La Barbera, Cyrille Collin, Lola Lilensten, Denis Jouaffre, Eric Markiewicz, Laurent Dubar

### ► To cite this version:

Benjamin Zielinski, Tarik Sadat, Rudy Dubois, José La Barbera, Cyrille Collin, et al.. Interface Characterization by Nanoindentation and EBSD of Cu/Cu and Al/Cu Joints Produced by Magnetic Pulse Welding (MPW). Proceedings of the 14th International Conference on the Technology of Plasticity - Current Trends in the Technology of Plasticity. ICTP 2023, 3, Springer Nature Switzerland, pp.53-63, 2024, Lecture Notes in Mechanical Engineering, 978-3-031-41341-4. 10.1007/978-3-031-41341-4\_7. hal-04279006

**HAL Id: hal-04279006**

**<https://hal.science/hal-04279006>**

Submitted on 10 Nov 2023

**HAL** is a multi-disciplinary open access archive for the deposit and dissemination of scientific research documents, whether they are published or not. The documents may come from teaching and research institutions in France or abroad, or from public or private research centers.

L'archive ouverte pluridisciplinaire **HAL**, est destinée au dépôt et à la diffusion de documents scientifiques de niveau recherche, publiés ou non, émanant des établissements d'enseignement et de recherche français ou étrangers, des laboratoires publics ou privés.



Distributed under a Creative Commons Attribution 4.0 International License

# Interface characterization by nanoindentation and EBSD of Cu/Cu and Al/Cu joints produced by Magnetic Pulse Welding (MPW)

Benjamin ZIELINSKI<sup>1</sup> \*, Tarik SADAT<sup>1</sup>, Rudy DUBOIS<sup>1</sup>, José LA BARBERA<sup>1</sup>,  
Cyrille COLLIN<sup>2</sup>, Lola LILENSTEN<sup>3</sup>, Denis JOUAFFRE<sup>4</sup>, Eric MARKIEWICZ<sup>1</sup>,  
Laurent DUBAR<sup>1</sup>

<sup>1</sup> Univ. Polytechnique Hauts-de-France, CNRS, UMR 8201 - LAMIH - Laboratoire d'Automatique de Mécanique et d'Informatique Industrielles et Humaines, F-59313 Valenciennes, France

<sup>2</sup> Mines ParisTech, Centre de Mise en Forme des Matériaux (CEMEF), UMR CNRS, PSL University, 1 rue Claude Daunesse, CS 10207, Sophia Antipolis, France

<sup>3</sup> PSL Research University, Chimie ParisTech-CNRS, Institut de Recherche de Chimie Paris, Paris, France

<sup>4</sup> PFT Innovaltech - Lycée Condorcet, Saint-Quentin, France  
benjamin.zielinski@outlook.com

\* Corresponding Author

## Abstract:

Magnetic Pulse Welding (MPW) is a high-velocity impact welding technique that allows the joining of dissimilar materials such as aluminium and copper. Welding should be produced under the appropriate conditions: impact velocity (200-500 m.s<sup>-1</sup>) and collision angle (10–30°). The formation mechanisms leading to the welding creation are not very clear. This work investigates the microstructure and hardness at the interface to understand these mechanisms.

Al/Cu and Cu/Cu samples were formed with identical process parameters. They were first compared to the literature using Vickers microhardness. Obtained results are standard and correspond to previous studies. In a second step, a detailed characterization of the interface using nanoindentation and electron back-scattered diffraction (EBSD) methods is done.

Different behaviors were found at the interface between Al/Cu and Cu/Cu. Al/Cu exhibited a thin layer of intermetallic compounds (IMC), increasing the hardness at the interface. This layer was composed of Al<sub>2</sub>Cu and Al<sub>4</sub>Cu<sub>9</sub> compounds, as demonstrated by Energy Dispersive Spectroscopy (EDS) and X-ray Diffraction (XRD). Cu/Cu presented a dissimilar behavior at the interface. The flyer sheet shows an increase in hardness due to grains deformation and distortion. While, the base sheet manifested a decrease in hardness caused by dynamic recovery or recrystallization at the interface. In both cases, the samples were deformed and hardened due to the plastic deformation induced during impact. These results are complementary to previous studies. They provide new insights that could be used to improve our understanding of the mechanisms behind such high-velocity impact welding.

**Keywords:** Microstructure, Magnetic Pulse Welding, Nanoindentation, Welding interface, Plastic deformation, Intermetallics

## 1 Introduction

Nowadays, structural components made of welded joints must combine various properties to ensure a high strength under complex and severe loadings while being lightweight. In order to combine these properties, different materials can be used simultaneously. However, usual welding techniques are mainly efficient to join similar materials. With dissimilar metals the melting temperature between the two elements can be very different, leading to undesirable thermal effects such as an important Heat-Affected Zone (HAZ) or a large area of Intermetallic Compounds (IMC). Other welding techniques need to be used for the welding of dissimilar materials.

Among others, Magnetic Pulse Welding (MPW), also known as Electro-Magnetic Pulse Welding (EMPW), is adapted to join dissimilar materials such as Aluminum (Al) and Copper (Cu). It is categorized as a High-Velocity Impact Welding (HVIW) due to its impact velocity between a flying (flyer) and fixed (base) sheet during the process ( $200\text{-}500\text{ m}\cdot\text{s}^{-1}$ ) [1]. The accelerating energy of the flyer plate is supplied by an electric pulse through an inductor (coil). MPW is known to have a very limited HAZ at the interface between the two materials but they undergo severe plastic deformation especially at the interface [2]. Searchers investigated the link between the interfacial morphology and the global [3] or local [4] mechanical properties of the joints. The produced interface is inhomogeneous with specific features such as waves and vortexes. These features are assumed to be a key marker of the process. Different hypotheses were made to explain their formation, most known are based on the Kelvin-Helmholtz instability and shock-waves interaction [5]. Numerical investigations were also conducted to reproduce these features and demonstrate their mechanisms formation [6].

Previous works shown effects on the local microstructure of similar (Cu/Cu [1], Al/Al [7]) or dissimilar (Al/Fe [8], Al/Mg [9] or Al/Cu [10]) assemblies. However, there was no specific study on the literature exploring the link between local microstructure and mechanical properties of Al/Cu and Cu/Cu assemblies by comparing nanoindentation and microstructure maps at the interface. The comparison of these maps permits to collect complementary data at the interface.

This work presents the properties evolution of the materials on the meso-scale of the assembly and locally at the interface. An Al/Cu assembly is compared to a Cu/Cu one produced under the same conditions. Several differences are highlighted to explain the underlying mechanisms on the microstructure at the interface.

## 2 Materials and Methods

### 2.1 Welds Characteristics

During this study, two couples of materials were welded by MPW. A commercial 1050 aluminum sheet of 1 mm thickness has been welded on a commercial copper of 2 mm for the first one. The second couple is an assembly of 2 copper sheets of 1- and 2-mm thickness. The welding was performed on a PULSAR 25 kJ-9 kV device with a

690  $\mu\text{F}$  condenser and a theoretical frequency of 25 kHz at PFT Innovaltech in France. The process parameters used during welding are described in Table 1.

**Table 1** : MPW process parameters

	Cu/Cu assembly	Al/Cu assembly
Base plate (fixed plate)	Copper – 2 mm	Copper – 2 mm
Flyer plate (mobile plate)	Copper – 1 mm	Aluminum – 1 mm
Base strip sizing	98 x 30 mm	98 x 30 mm
Flyer strip sizing	98 x 30 mm	98 x 30 mm
Energy used (kJ)	19.4	19.4
Gap (mm)	2	2
Overlapping (mm)	7	7

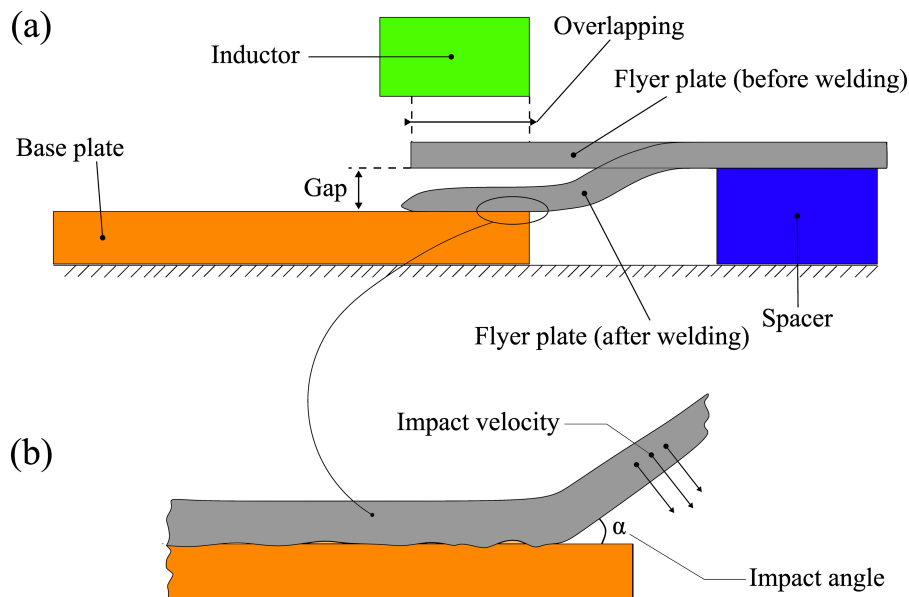


**Fig. 1** : Scheme for the MPW set-up and parameters; (a) – General view of the set-up, (b) – Impact velocity and angle orientation

Fig. 1a depicts the different elements from the MPW process as a schematic figure with their position and localizations. Fig. 2 displays Cu/Cu and Al/Cu samples after welding. The global aspect of the assemblies is different between the Al/Cu and Cu/Cu samples because of the materials properties. Aluminum sheet is more deformed and twisted than the copper one due to lower mechanical properties. It is important to note that the impact angle and velocity (described in Fig. 1b) between Al/Cu and Cu/Cu are not identical. This is linked with their different electric properties, hence leading to a different magnetic field.

## 2.2 Sample preparation

Welded samples were cut in perpendicular cross-section of the welding seam to extract sub-samples and to study the welding seam at the interface. An example of the cross-section orientation is shown on Fig. 2. Cutting was performed using a Secotom-10 (Struers) device. Then, the sub-samples were mounted using a CitroPress-5 (Struers) and polished by a Tegramin-25 (Struers).

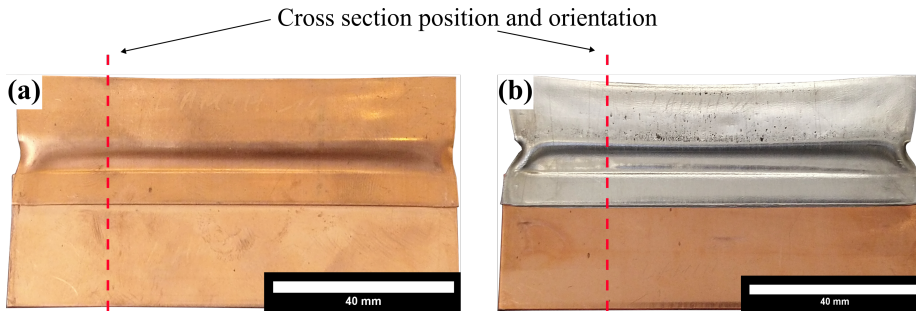


**Fig. 2 :** Aspect of the samples after welding and example of cross-section direction; (a) - Cu/Cu, (b) – Al/Cu.

Different polishing protocols were used on the sub-samples depending of the assembly. For Cu/Cu, standard polishing was executed with Silicon Carbide (SiC) paper up to Grit 2000, then it was electro-polished using a LectroPol-5 (Struers) device. This protocol permits to reach very good surface preparation allowing to use nanoindentation and Electron Back-Scattered Diffraction (EBSD) techniques on the Cu/Cu samples.

For Al/Cu samples a different protocol should be used because it is not possible to achieve a good electropolishing on both surfaces simultaneously. The samples were polished with standard SiC papers up to Grit 2000, followed by 3, 1 and 0.25  $\mu\text{m}$  diamonds solutions sprayed on different cloths in order to obtain mirror finish samples. A final step was realized with colloidal silica solution. While the surface quality preparation was sufficient for nanoindentation, there was scratches present that make EBSD analysis difficult. Therefore, a different protocol owed to be used. 3 mm cubic pieces were extracted from welding using Wire Electrical Discharge Machining (WEDM). These pieces were then ionic polished using an EM TIC 3X ionic beam milling system (Leica).

## 2.3 Characterization Methods

Samples were analyzed using different characterization techniques to obtain several complementary information. Mechanical characterization was performed using a microhardness indenter and a nanoindenter.

Micro-hardness testing was carried out using a micro-hardness testing machine from Future Tech with a motor driven stage. Hardness was measured using a Vickers indenter operating at 50 gf / 15 s according to ASTM E384-17 [11]. The distance

between each indent was 150  $\mu\text{m}$ . Nano-hardness measurements were performed using a Hysitron TI980 (Bruker) device. Data were acquired using XPM mode (10 x 10 grid), which allowed ultra-fast indentation acquisition. The indents were made using 700  $\mu\text{N}$  with a spacing distance of 3.5  $\mu\text{m}$  for Al/Cu and 2  $\mu\text{m}$  for Cu/Cu. The use of these two techniques allowed to get global and local information on the mechanical properties of the sample.

Welding microstructure was studied using Scanning Electron Microscopy (SEM) images and EBSD. Analyses were conducted using two apparatus, a JSM 7100F (Jeol) and a Supra 40 (Zeiss) devices due to the different samples' preparation protocols.

### 3 Results & Discussions

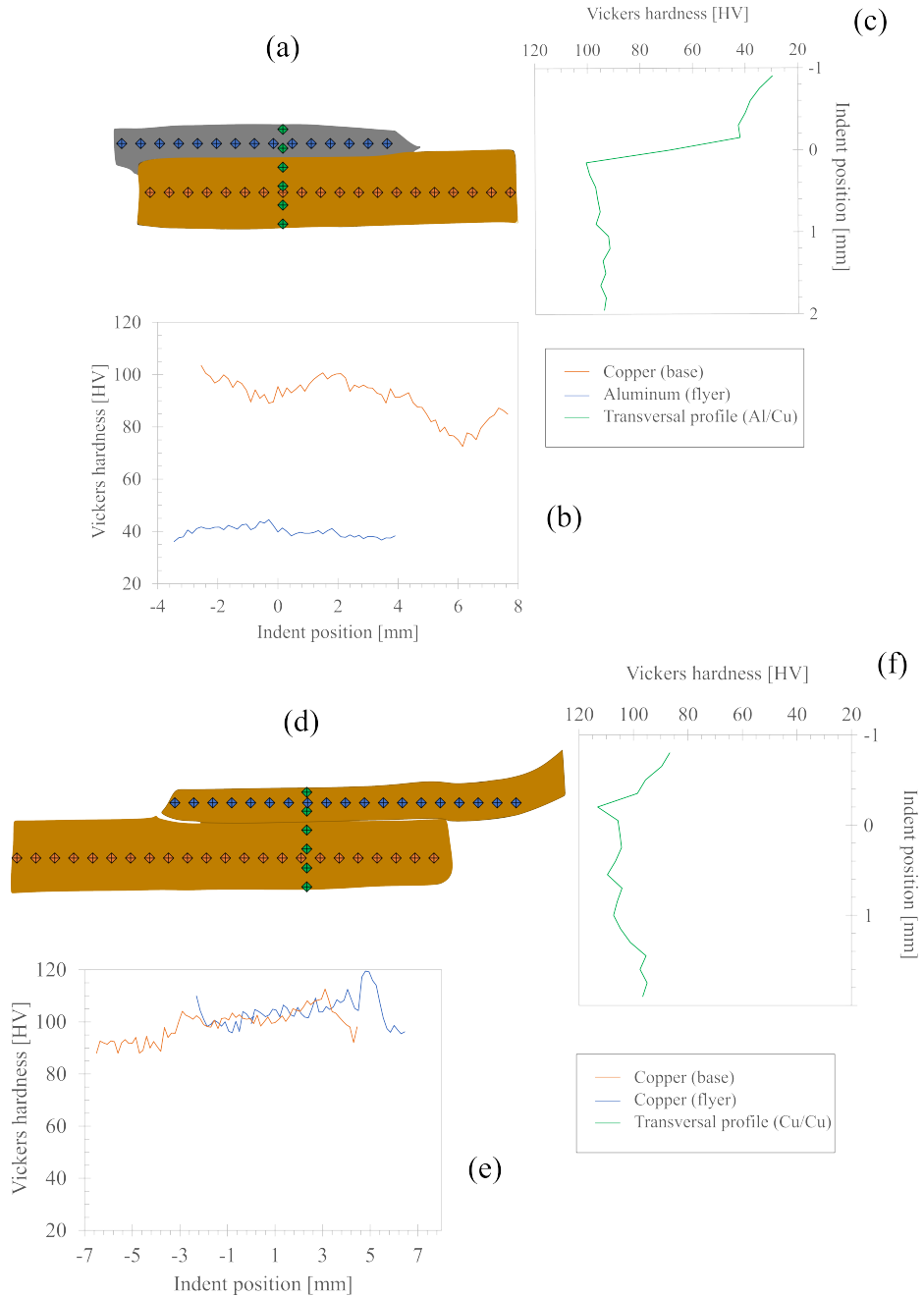
Interface characterization was performed on Cu/Cu and Al/Cu samples produced with the same process parameters (see Table 1).

#### 3.1 Micro-hardness

Micro-hardness was used to obtain global information on the welds and a reference to allow a comparison with previous studies.

Fig. 3 shows the measurements locations taken during this work. Longitudinal profiles were done at half the thickness of each plate. The Al/Cu sample exhibited a significant gradient at the interface due to the use of dissimilar materials during the welding process. These results are in agreement with previous works, particularly for the copper hardness [10]. The Cu/Cu sample demonstrated a slight increase in hardness on the welding area compared to the external part of the base plate indicating a plastic hardening of the sample. This finding is consistent with a previous study done on Al/Al welding [12].

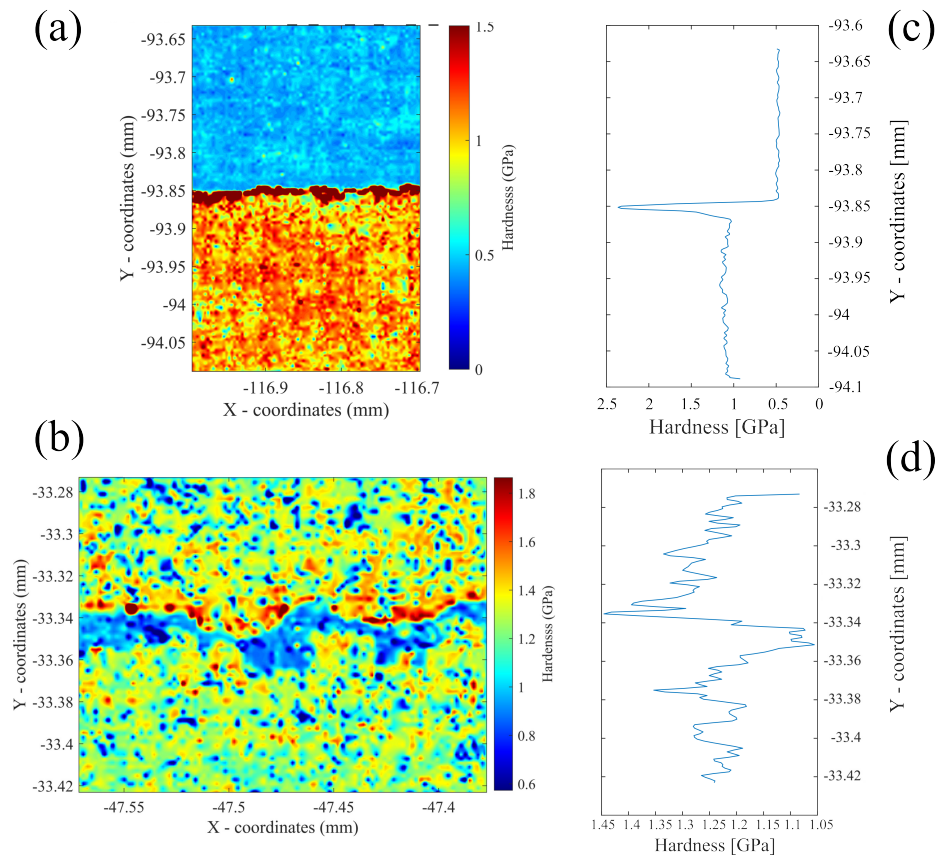
It is important to note that intermetallic compounds (IMC) hardness were not visible in the results due to the large prints size (around 35  $\mu\text{m}$  diagonal on the copper side and 48  $\mu\text{m}$  for the aluminum side) compared to the thin thickness of the IMC layer (between 5-20  $\mu\text{m}$ ). However, it can be seen that the copper base plate was more hardened with the Cu/Cu assembly. These measurements were conventional and with expected outcome. Although, they indicate that the samples examined are comparable to those studied in the literature.



**Fig. 3 :** Longitudinal and transversal microhardness Vickers for Al/Cu and Cu/Cu welds; (a) and (d) – Al/Cu and Cu/Cu schemes with the measurement locations; (b) and (e) – Longitudinal measurements on Al/Cu and Cu/Cu samples; (c) and (f) Transversal profile on Al/Cu and Cu/Cu samples.

### 3.2 Nano-indentation

Second step of the characterization was to study locally the hardness across the interface for Al/Cu and Cu/Cu samples using nanoindentation.



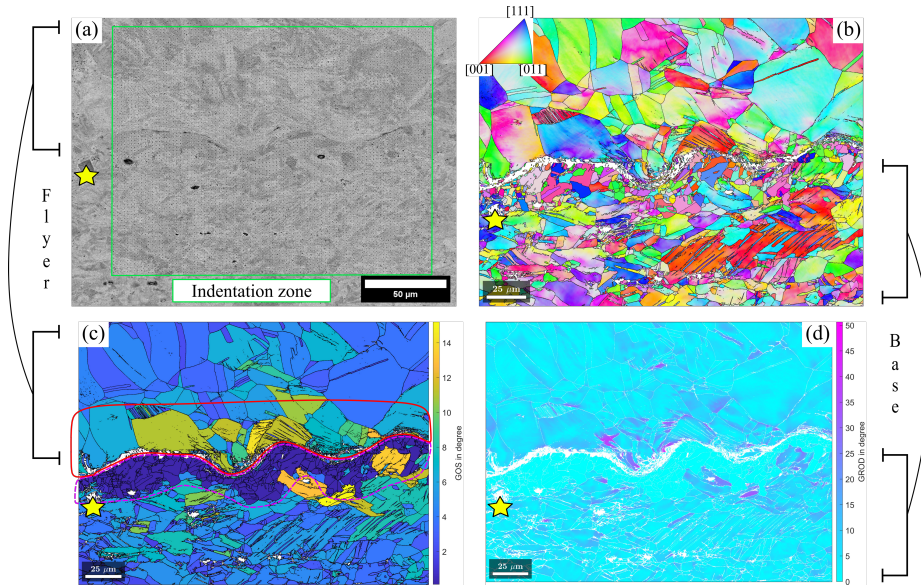
**Fig. 4 :** Nano-indentation hardness maps and average profile lines, (a) and (b) – Hardness maps for Al/Cu and Cu/Cu, (c) and (d) – Average hardness values along the Y-axis.

Fig. 4 shows the nanoindentation maps obtained for Al/Cu and Cu/Cu. The behavior between the two components was different. In the Al/Cu case, there was an important increase of the hardness at the interface as a result of the presence of IMC (as shown in the following subsection). No effects were measured beyond 10-15  $\mu\text{m}$  around the interface. The Cu/Cu nanoindentation map was different, it presented a reduction in the hardness on one side of the interface and an increase of the hardness on the other side. The impacted zone around the interface was slightly bigger than the Al/Cu sample.

Additional characterization was performed to understand the origin of these variations.

### 3.3 SEM & EBSD

SEM allows us to get complementary information to those previously collected. Visualization can help to understand and explain the different variations obtained.



**Fig. 5** : SEM and EBSD images - Cu/Cu sample, (a) – BSE image of the EBSD location with annotations, (b) IPF map, (c) GOS map, (d) GROD map

Cu/Cu sample was observed under SEM, it presented a wavy interface. The Microstructure from the flyer and base plates were different due to their distinct production conditions. The average grain diameter from the flyer was  $10.5 \mu\text{m}$  compared to  $5.4 \mu\text{m}$  from the base plate.

A micro-indentation was made at the interface to be used as a marker during the EBSD / nano-indentation, it is represented under the yellow star in Fig. 5. Fig. 5a display the location where the Cu/Cu nano-indentations testing was performed compared to the EBSD map. The grains from the flyer part were heavily deformed close to the interface. This can be observed on the Inverse Pole Figure (IPF) (Fig. 5b) map where the grains have an internal gradient of colors. This distortion can also be computed by the Grain Orientation Spread (GOS) (Fig. 5c) map, which is the average misorientation angle of a grain compared to its mean orientation. The more deformed grains are surrounded by the red shape (continuous line) in Fig. 5c. This can be enhanced by using the Grain Reference Orientation Deviation (GROD) (Fig. 5d) map. It is evaluating the misorientation from a local point of a grain to its mean orientation. The work has been carried out using the MTEX toolbox [13] available with

MATLAB. GOS and GROD maps provide local information about deformation of grains, and can be used to study the recovery and recrystallization of materials [14]. They differ from the IPF map, which indicates grain orientation.

We also found that grains from the base plate (just below the interface) were at the opposite without any distortion. They had a GOS or GROD measurements equal to zero. They are visible inside the purple shape (dashed line) in Fig. 5c. This may be a mark of dynamic recovery or recrystallization that occurred during the welding process. This explains the hardness drop measured during the nano-indentation due to the limited quantity of distortion at this localization.

As explained previously in 2.2 Sample preparation, it was not possible to execute nano-indentation and EBSD on the same location for Al/Cu. Another sample was used.

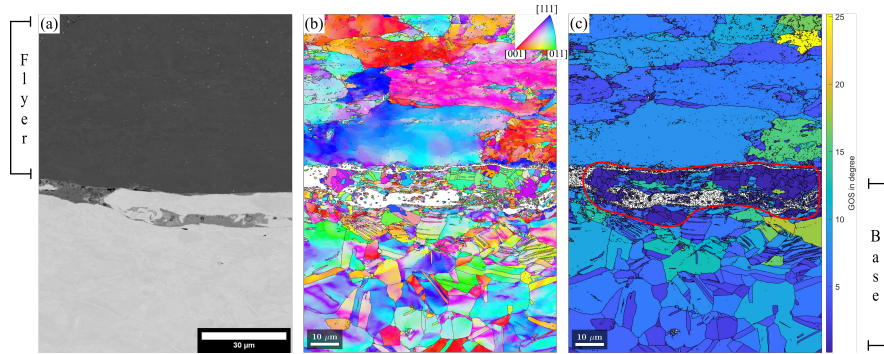


**Fig. 6** : SEM and EBSD images - Al/Cu sample, (a) – SE image of the EBSD location, (b) IPF map, (c) GOS map

Fig. 6 shows the microstructure characterization for Al/Cu sample. It is interesting to note that the interface presents also dynamic recovery or recrystallization marks (red shape in Fig. 6c). However, the impacted area is reduced compared to Cu/Cu. Both sides have grains highly deformed. Copper grains (bottom side) are heavily twinned for both welding cases, whereas aluminum grains are not (top side). This agrees with the literature and the aluminum high stacking-fault energy [15].

IMC compounds were not indexed during the EBSD characterization due to poor signal. They correspond to the white areas on Fig. 6b and Fig. 6c. Energy dispersive spectroscopy (EDS) and X-ray diffraction (XRD) were used to characterize these IMCs. Room temperature X-ray diffraction (XRD) measurements were conducted using a Cu-K $\alpha$  radiation ( $\lambda = 0.15406$  nm) X'Pert PRO PANalytical instrument. Two IMCs were found that correspond to Al<sub>2</sub>Cu and Al<sub>4</sub>Cu<sub>9</sub> (see Fig. 7).

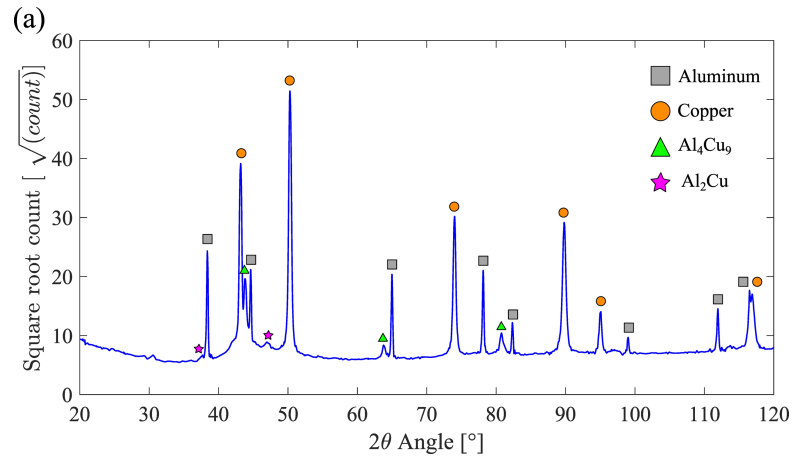


Fig. 7 : Al/Cu XRD diffractogram

## 4 Conclusion

Al/Cu and Cu/Cu assemblies were produced by MPW using identical process parameters. They were compared to the literature using Vickers microhardness and they show standard hardness measurements. Then, they have been locally characterized at the interface to highlight the local evolution in this area.

The Al/Cu and Cu/Cu samples demonstrated different behaviors and mechanisms. Cu/Cu showed the creation small grains at the interface with a dissimilar behavior on both sides. The area of the flyer part close to the interface increased its hardness due to grain distortion. On the other hand, the close interface area from the base part had a reduction in hardness due to dynamic recovery or recrystallization of grains during the welding.

The Al/Cu samples did not present these characteristics on the same scale. The dynamic recovery or recrystallization area were more reduced compared to Cu/Cu. However, two IMCs compounds were found at the interface, which they locally affected the hardness by increasing it.

## 5 References

1. Zhang Y, Babu SS, Daehn GS (2010) Interfacial ultrafine-grained structures on aluminum alloy 6061 joint and copper alloy 110 joint fabricated by magnetic pulse welding. *J Mater Sci* 45:4645-4651. <https://doi.org/10.1007/s10853-010-4676-0>
2. Kapil A, Sharma A (2015) Magnetic pulse welding: An efficient and environmentally friendly multi-material joining technique. *J Clean Prod* 100:35-58. <https://doi.org/10.1016/j.jclepro.2015.03.042>
3. Kwee I, Faes K (2016) Interfacial Morphology and Mechanical Properties of Aluminium to Copper Sheet Joints by Electromagnetic Pulse Welding. *Key Eng Mater* 710:109-114. <https://doi.org/10.4028/www.scientific.net/KEM.710.109>

4. Zielinski B, Sadat T, Lukić B, et al (2023) Characterization of local mechanical properties of Al/Cu Magnetic Pulse Welded joints under high strain rates using synchrotron X-ray imaging. *Mater Lett* 337:.. <https://doi.org/10.1016/j.matlet.2023.133943>
5. Ben-Artzy A, Stern A, Frage N, et al (2010) Wave formation mechanism in magnetic pulse welding. *Int J Impact Eng* 37:397-404. <https://doi.org/10.1016/j.ijimpeng.2009.07.008>
6. Li JS, Sapanathan T, Raoelison RN, et al (2021) On the complete interface development of Al / Cu magnetic pulse welding via experimental characterizations and multiphysics numerical simulations. *J Mater Process Technol* 296:.. <https://doi.org/10.1016/j.jmatprotec.2021.117185>
7. Raoelison RN, Sapanathan T, Buiron N, Rachik M (2015) Magnetic pulse welding of Al/Al and Al/Cu metal pairs: Consequences of the dissimilar combination on the interfacial behavior during the welding process. *J Manuf Process* 20:112-127. <https://doi.org/10.1016/j.jmapro.2015.09.003>
8. Cui J, Sun T, Geng H, et al (2018) Effect of surface treatment on the mechanical properties and microstructures of Al-Fe single-lap joint by magnetic pulse welding. *Int J Adv Manuf Technol* 98:1081-1092. <https://doi.org/10.1007/s00170-018-2262-9>
9. Chen S, Jiang X (2015) Microstructure evolution during magnetic pulse welding of dissimilar aluminium and magnesium alloys. *J Manuf Process* 19:14-21. <https://doi.org/10.1016/j.jmapro.2015.04.001>
10. Wang PQ, Chen DL, Ran Y, et al (2020) Electromagnetic pulse welding of Al/Cu dissimilar materials: Microstructure and tensile properties. *Mater Sci Eng A* 792:139842. <https://doi.org/10.1016/j.msea.2020.139842>
11. ISO/ASTM International (2017) E384 – 17: Standard Test Method for Microindentation Hardness of Materials
12. Li Z, Beslin E, den Bakker AJ, et al (2020) Bonding and microstructure evolution in electromagnetic pulse welding of hardenable Al alloys. *J Mater Process Technol* 290:116965. <https://doi.org/10.1016/j.jmatprotec.2020.116965>
13. Bachmann F, Hielscher R, Schaeben H (2011) Grain detection from 2d and 3d EBSD data-Specification of the MTEX algorithm. *Ultramicroscopy* 111:1720-1733. <https://doi.org/10.1016/j.ultramic.2011.08.002>
14. Carneiro Í, Simões S (2020) Recent advances in ebsd characterization of metals. *Metals (Basel)* 10:1-32. <https://doi.org/10.3390/met10081097>
15. Chen S, Wang Q, Liu X, et al (2020) First-principles studies of intrinsic stacking fault energies and elastic properties of Al-based alloys. *Mater Today Commun* 24:101085. <https://doi.org/10.1016/j.mtcomm.2020.101085>